SUPPLEMENTAL INFORMATION

A Requirement for ERK dependent Dicer Phosphorylation in Coordinating Oocyte-to-Embryo Transition in *Caenorhabditis elegans*

Melanie Drake[1], Tokiko Furuta[1], Kin Suen Man[2,3], Gabriel Gonzalez[1,3], Bin Liu[4], Awdhesh Kalia[5], John Ladbury[2, 3], Andrew Z. Fire[6], James B Skeath[7], Swathi Arur[1, 3, 4*]

1: Department of Genetics, UT MD Anderson Cancer Center, Houston, TX, 77030, USA

2: Department of Biochemistry and Molecular Biology, UT MD Anderson Cancer Center, Houston, TX, 77030, USA

3: Graduate School of Biomedical Sciences, Houston, TX, 77030, USA

4: Center for Genetics and Genomics, UT MD Anderson Cancer Center, Houston, TX, 77030, USA

5. Graduate Program in Diagnostic Genetics, School of Health Professions, UT MD Anderson Cancer Center, Houston, TX, 77030, USA

6: Department of Pathology and Genetics, Stanford University, Stanford, CA, 94305, USA

7: Department of Genetics, Washington University School of Medicine, Scott Avenue, Saint Louis, MO, 63110, USA

*Address correspondence to:
Swathi Arur, Ph.D

Department of Genetics

Unit 1010

UT MD Anderson Cancer Center

Houston, 77030

Phone: 713-745-8424

Email: sarur@mdanderson.org

SUPPLEMENTAL DATA.

Drake et al., Figure S1

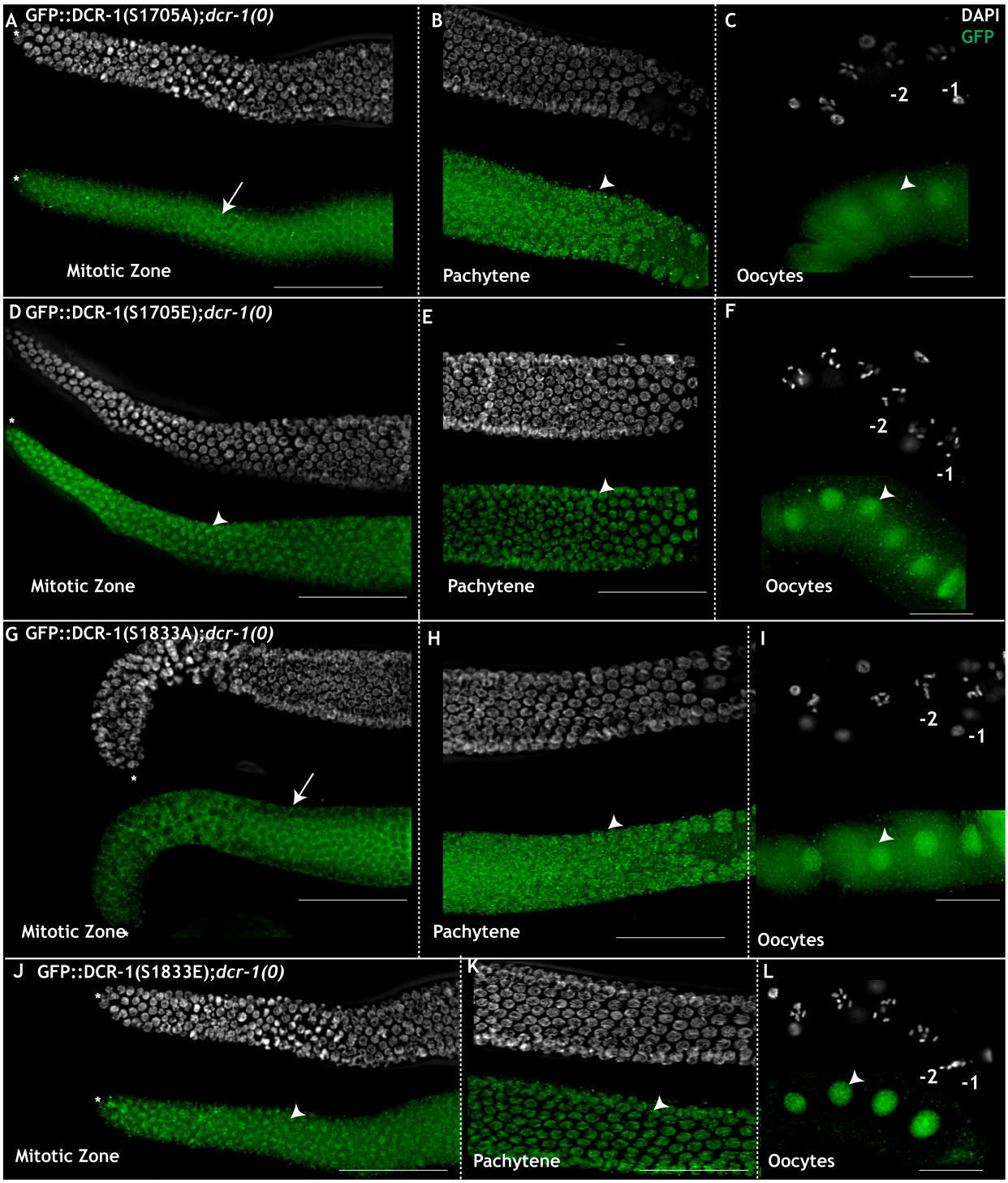

Figure S1: Phosphorylation of Dicer is necessary and sufficient for nuclear translocation. (See also Figure 3)

A-C: Expression of GFP::DCR-1(S1705A) in *dcr-1(0)* adults exhibits cytoplasmic localization in mitotic cells (arrowhead, A), cytoplasmic and nuclear (double arrow) in pachytene (B) and oocytes (C). **D-F:** Expression of GFP::DCR-1(S1705E) in *dcr-1(0)* exhibits nuclear localization (double arrows) in mitotic cells (D), pachytene (E) and oocytes (F). **G-I**: Expression of GFP::DCR-1(S1833A) in *dcr-1(0)* exhibits cytoplasmic localization (arrow heads) in mitotic and cytoplasmic and nuclear localization in pachytene cells (H) and oocytes (I). **J-L**: Expression of GFP::DCR-1(S1833E) in *dcr-1(0)* exhibits nuclear localization (double arrows) in mitotic cells (J), pachytene cells (K) and oocytes (L). Scale bar: 40 μm.

Drake *et al.*, Figure S2

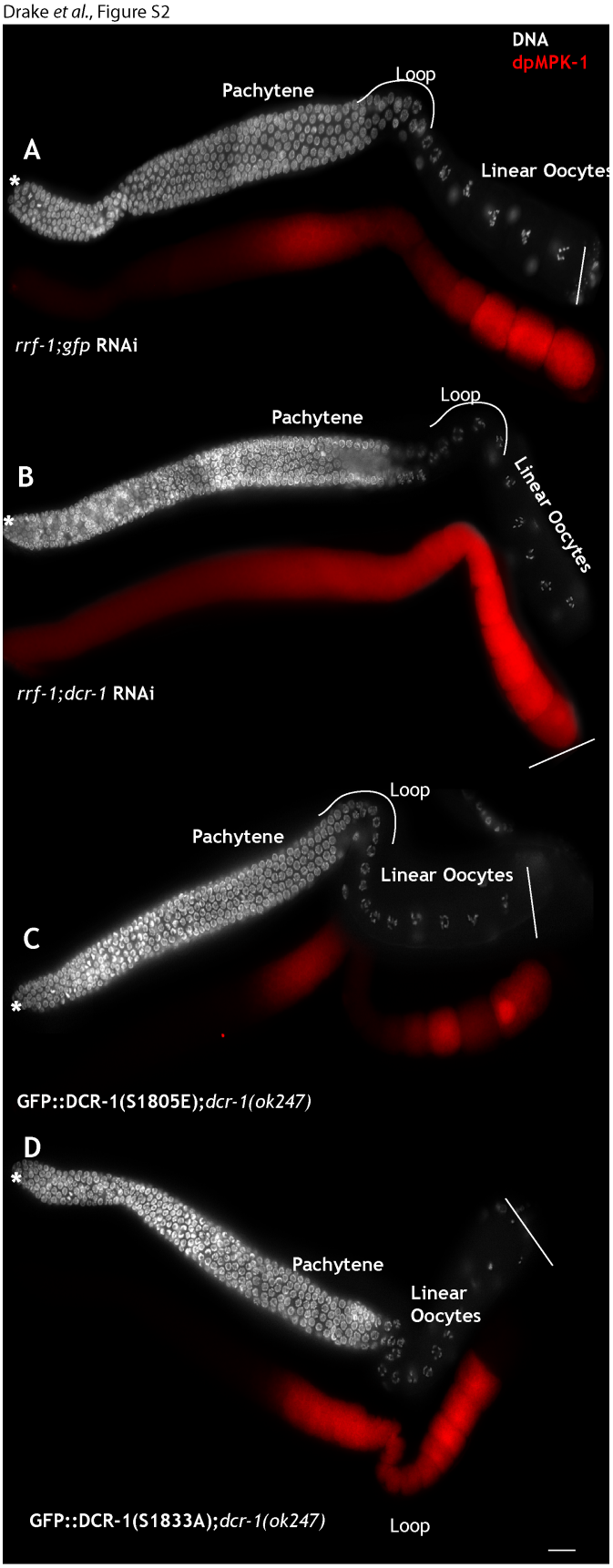

Figure S2: Lack of phosphorylation of DCR-1 at 1833 results in ectopic activation of MPK-1 ERK in the germline. (See also Figure 5)

Dissected adult *C. elegans* hermaphroditic germlines oriented left to right. Left: Distal tip cell (asterisk), right: oocytes. **A** *rrf-1* animals treated with either gfp RNAi and (**B**) *dcr-1* RNAi stained with DAPI (white) to visualize DNA and dpMPK-1 (red) to visualize active MPK-1. **C**: Expression of GFP::DCR-1(S1833E) transgene in an otherwise *dcr-1(0)* background restores normal dpMPK-1 accumulation in the loop region. **D**: Expression of GFP::DCR-1(S1833A) transgene in an otherwise *dcr-1(0)* background results in the development of fertile animals with morphologically normal oocytes, and ectopic activation of MPK-1 in the loop region.

Drake *et al.*, Figure S3

A GFP::DCR-1 transgenes generated by Biolistic Transformation

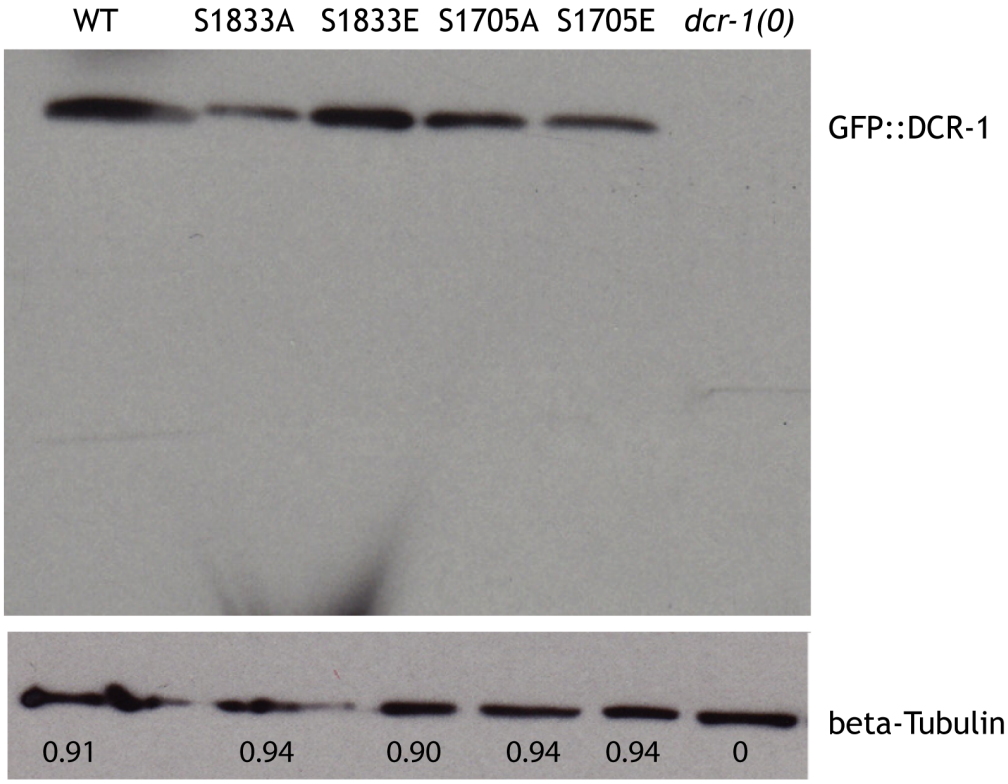

B GFP::DCR-1 transgenes generated via MosSci

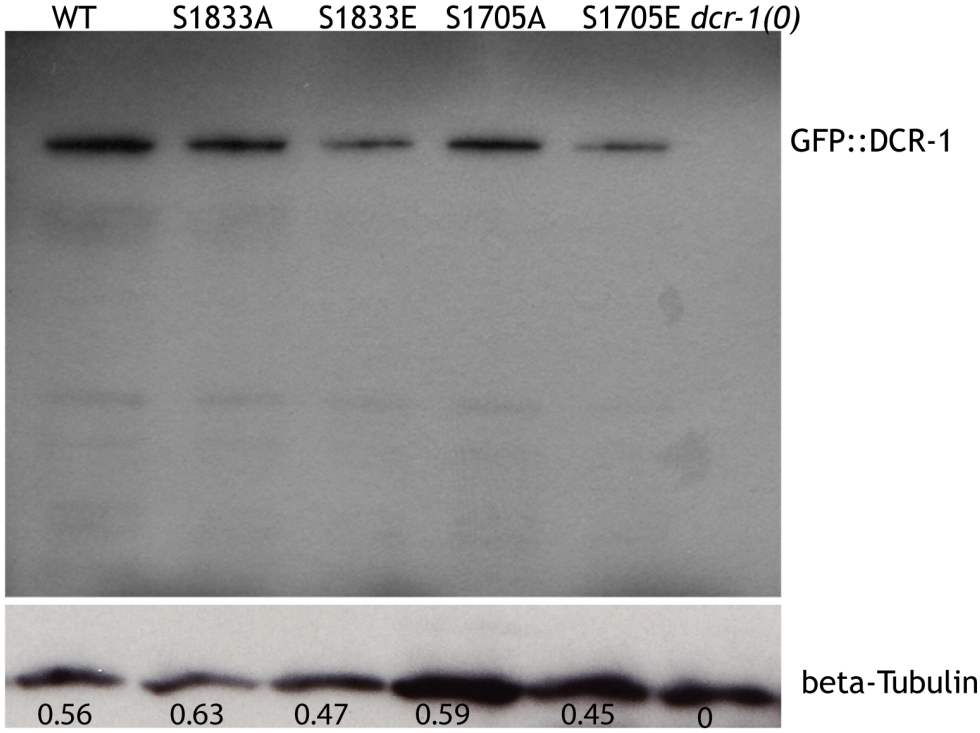

Figure S3: GFP::DCR-1 wild type and mutant transgenes express at similar levels. (See also Figure 6)

200 homozygous animals from each of the DCR-1 transgenic (WT, S1705A S1705E, S1833A, S1833E) as well as *dcr-1(0)* background were lysed in 2X SDS sample buffer and resolved on a 8% SDS PAGE, and probed with either GFP antibody (panels A and C) or tubulin (panels B and D). GFP antibody recognizes ~ 220 kDa band at similar intensity in each of the transgenes, which is absent from the null. Tubulin, the loading control. Image J analysis to quantify the fold accumulation of DCR-1 GFP levels relative to the tubulin control are indicated as numbers below the tubulin panel.

Drake *et al.*, Fig. S4

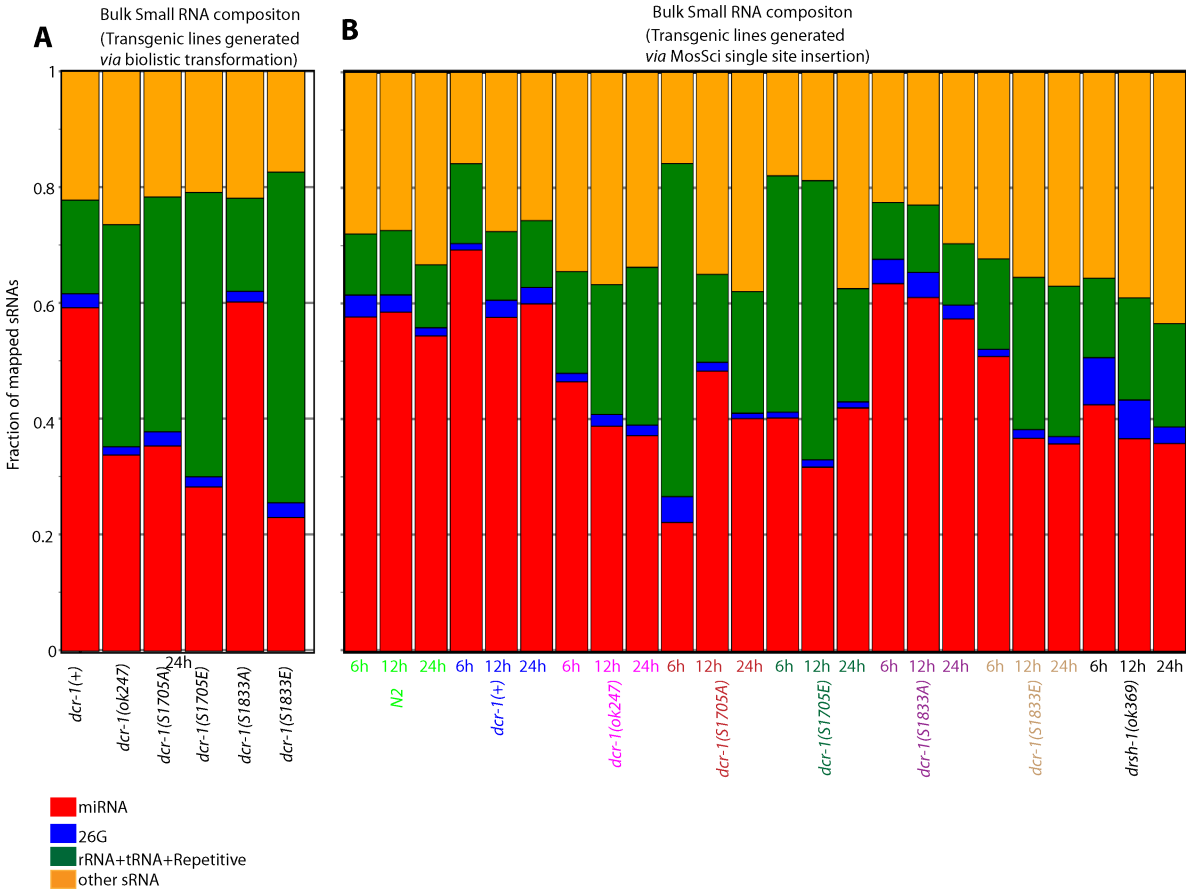

Figure S4. Overall makeup of small RNA populations from wild type, mutant, and transgene-rescued populations. (See also Figure 6)

Animals were hand picked and synchronized at the L4/Adult molt. For mutant and transgene-rescued strains, populations were homozygotes for *(dcr-1(ok247)* at the chromosomal locus that were derived from a fertile *dcr-1(+)/dcr-1(ok247)* heterozygote parent. Small RNA sequences were obtained through direct ligation, selecting for molecules with a simple 5'-monophosphate terminus [Pak et al., 2006]). Proportions of total RNAs in the 20-30 size range (inclusive) that can precisely map to the *C. elegans* ws220 genome assembly are reported. miRNA species are all precise matches to miRNAs from miRbase, 26G RNAs are all RNAs of 26nt with a 5' G, repetitive+rDNA+tRNA are all reads matching the rDNA cluster, known tRNAs, or matching repeated regions of the genome. **A**: Distribution of small RNAs in an independent set of transgenic strains created by bombardment (biolistic transformation). **B** Distribution of transgene strains integration by mos-sci (Methods).

Drake *et al.*, Fig. S5

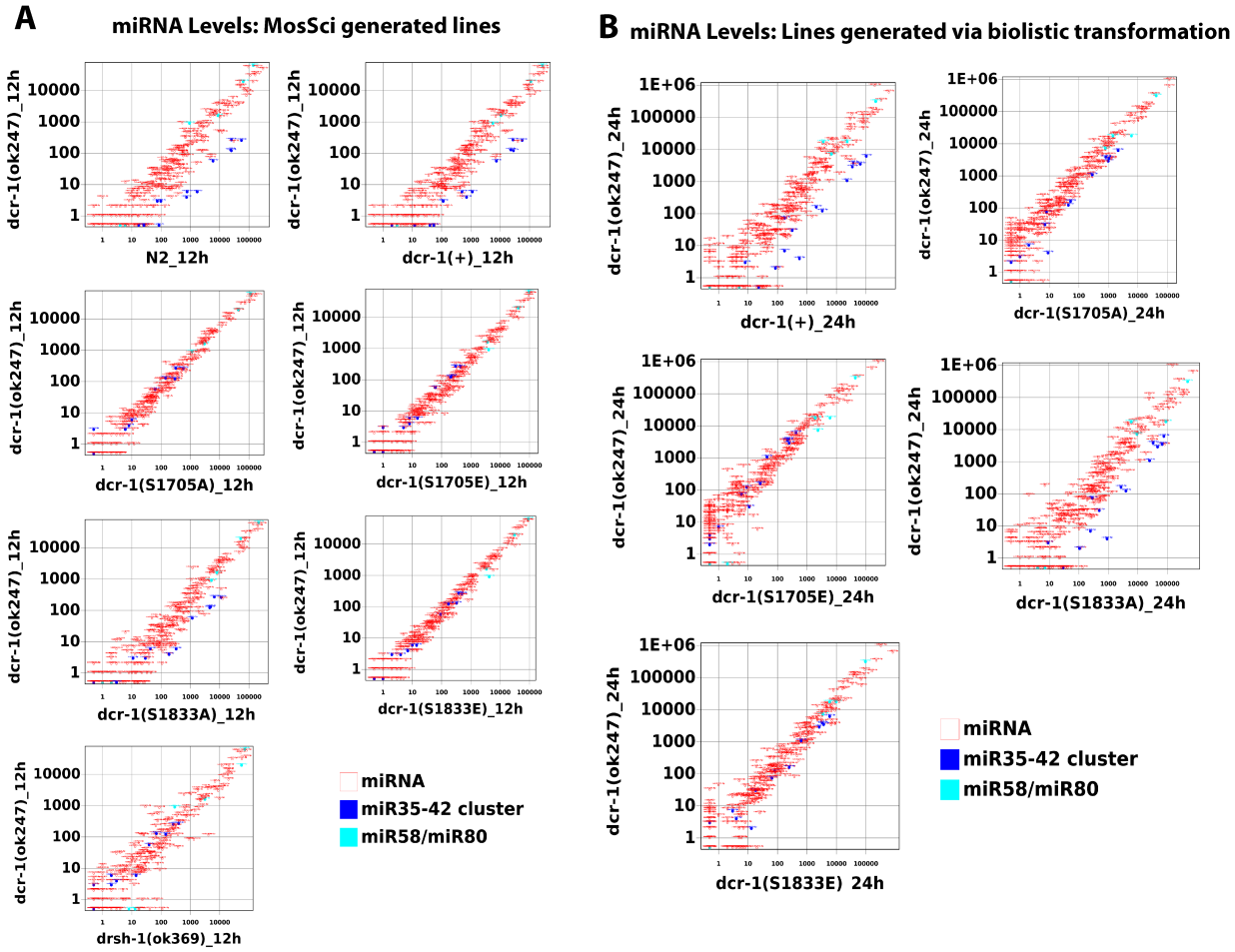

Figure S5: Comparisons of individual miRNA abundances. (See also Figure 6)

Samples are as in Figure S3. Counts from each miRNA were determined and a point is placed on the two dimensional canvas with the X and Y coordinates corresponding to the abundance in the two strains shown. miRNAs from cluster miR35-42 are shown in blue, with miR58 and miR80 products in orange. **A**: shows how transgenic strains obtained using Mos-Sci integration at 12 hr post L4-Adult molt (similar patterns are observed at 6 and 4 hr, data not shown). **B:** show transgenic strains obtained using Biolistic transformation (bombardment) at 24hrs past L4.

Drake *et al.*, Fig. S6

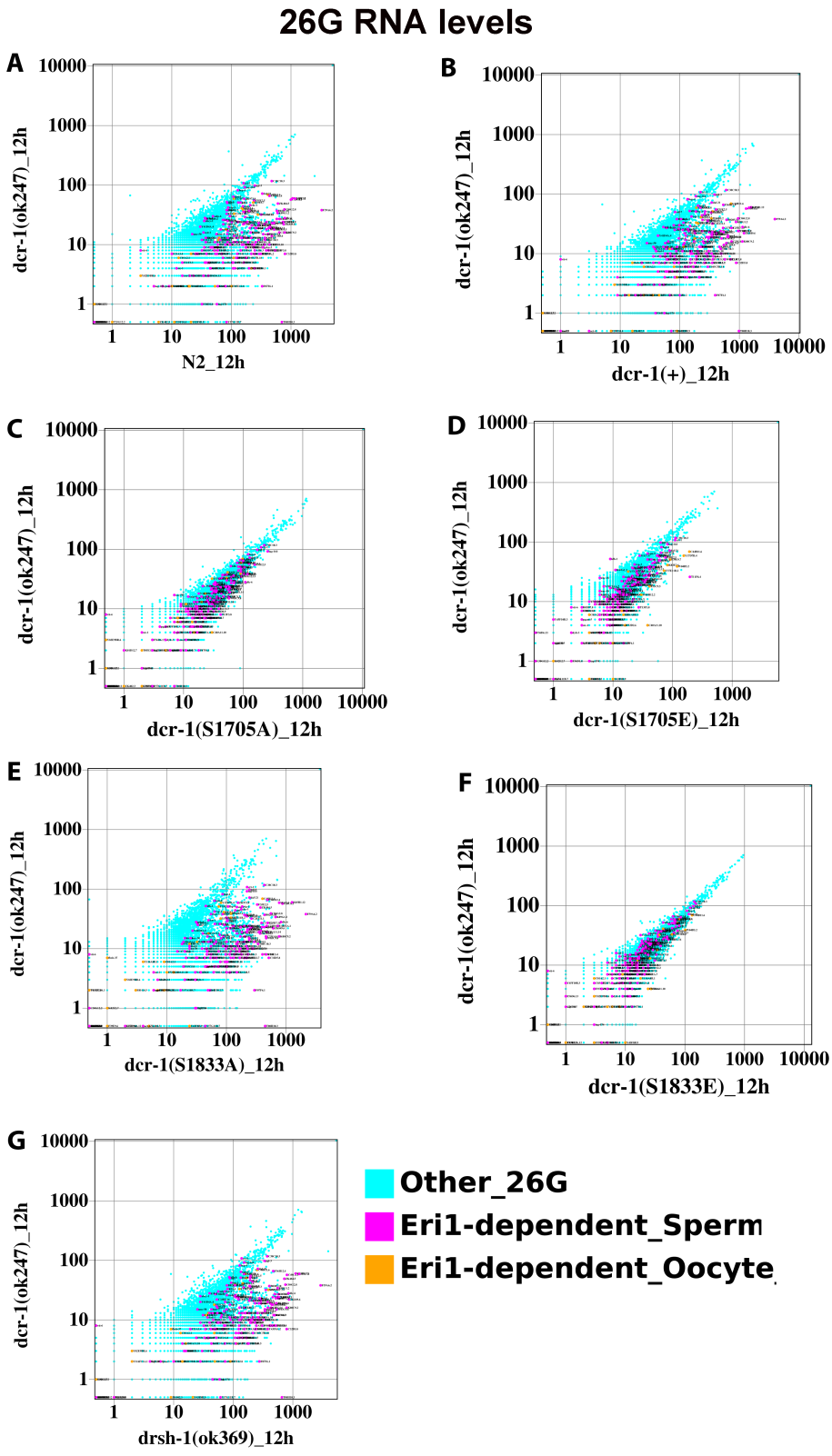

Figure S6: Phosphorylation of Dicer impairs its activity towards generation of 26G endo-siRNAs. (See also Figure 6)

Scatter plots depicting 26G RNA counts for individual genes, with comparisons in each case between the indicated mutant background and *dcr-1(ok247null)* populations. A subset of unique 26G RNA targets have been classified as sperm dependent (red), or oocyte dependent (blue), based on their observed incidence in samples as described by Han et al. (2009). **A**: The DCR-1 WT transgene rescues both the Class I and Class II 26G RNAs in young adult animals. **B**: Animals carrying a non-phosphorylatable 1833 DCR-1 transgene mimic the wild-type pattern (compare A to B), while (**C**) phospho-mimetic 1833 DCR-1 transgene, **D**: Non-phosphorylatable 1705 DCR-1 transgene, and **E**: phospho-mimetic 1705 DCR-1 transgene produce a similar loss of 26G RNAs to that seen in *dcr-1(0)*. **F**: Loss of DROSHA does not impact the production of 26G RNAs. These plots are derived from 12 hrs past L4 stage.

Drake *et al.*, Fig. S7

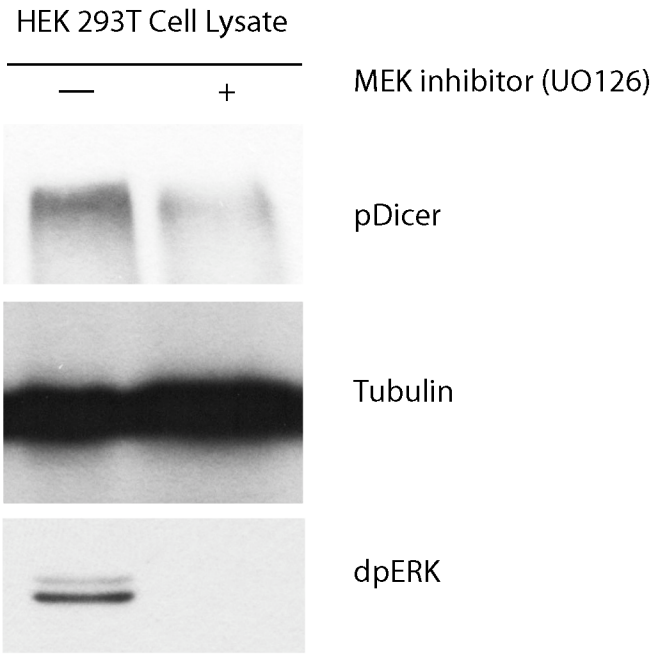

Figure S7: MEK Inhibition upon FGF stimulation, results in reduction of Dicer phosphorylation. (See also Figure 7)

HEK 293T cells were stimulated with FGF, to activate ERK, and simultaneously were treated with MEK inhibitor to inhibit ERK activation. Treatment with MEK inhibitor resulted complete abrogation in phosphorylation of ERK (lane 3), and a decrease in phosphorylation of Dicer (lane 1). Tubulin was used as the loading control.

TABLE S1: PHENOTYPES OF DCR-1 TRANSGENES GENERATED via MosSci BASED INTEGRATION

DCR-1 TRANSGENE	GENOTYPE	PHENOTYPES					
		Germline Development		dpMPK-1 Accumulation		Embryo Development	
	MosSci Transgenes	Phenotype	N (% with phenotype)	Phenotype	N (% with phenotype)	Phenotype	N (% with phenotype)
Null	*dcr-1(ok247)* III	Endomitotic oocytes	50 (100)	high dpMPK-1 in loop	50 (100)	None*	50 (100)
WT	[pDcr-1::gfp::dcr(WT)::dcr3'UTR] II;*unc-119(ed3) dcr-1(ok247)*	WT	76 (100)	WT (bimodal distribution of dpMPK-1 in the germline)	76 (100%)	WT, brood size (223)	76(100)
S1705E	[pDcr::gfp::dcr(1705E)::dcr3'UTR] II;*unc-119(ed3) dcr-1(ok247)*	WT (all oocytes in diakinesis)	87 (100)	WT (bimodal distribution)	87 (100%)	Embryonic lethal (before 30 cell stage)#	122 (100)
S1705A	[pDcr::gfp::dcr(1705A)::dcr3'UTR] II;*unc-119(ed3) dcr-1(ok247)*	Pachytene disorganization	71 (100)	low**	ND	Sterile	NA
		Polyploid pachytene nuclei	49 (15)	ND**	ND	NA	
		Disorganized oocytes	71 (100)	ND**	ND	NA	
S1705A/+	[pDcr::gfp::dcr(1705A)::dcr3'UTR]II;*unc-119(ed3) dcr-1(ok247)/ hT2GFP*	Pachytene disorganization	50 (86)	ND**	ND	WT, brood size (30-40) due to low level sterility	50 (95)
		Disorganized oocytes	50 (100)	ND**	ND		
		Polyploid pachytene nuclei	8 (16)	ND**	ND		
S1833E	[pDcr::gfp::dcr(1833E)::dcr3'UTR] II;*unc-119(ed3) dcr-1(ok247)*	WT	86 (100)	WT (bimodal distribution of dpMPK-1 in the germline)	86 (100)	Embryonic lethal (before 30 cell stage)#	101 (100)
S1833A	[pDcr::gfpdrc(1833A);;dcr3'UTR] II;*unc-119(ed3) dcr-1(ok247)*	WT	60 (87)	high dpMPK-1 in loop	60 (100)	WT, brood size (~180-200)	60 (100)
		Small oocytes	60 (13)	high dpMPK-1 in loop	60 (100)	Sterile	
S1705ES1833E	[pDcr::gfp::dcr(1705E1833E)::dcr3'UTR] II;*unc-119(ed3) dcr-1(ok247)*	WT (all oocytes in diakinesis)	32 (100)	WT (bimodal distribution of dpMPK-1 in the germline)	32 (100)	Embryonic Lethal#	55 (100)
S1705AS1833A	[pDcr::gfp::dcr(1705A1833A)::dcr3'UTR]*II;unc-119(ed3) dcr-1(ok247)*	Pachytene disorganization	45 (100)	ND**	ND	NA	
		Oocyte Disorganization	45 (100)	ND**	ND	NA	
		Polyploid pachytene nuclei	32 (71)	ND**	ND	NA	

See also Figures 3, 5 and 6

* The animals are sterile and produce no embryos

mothers carrying the embryos were cut open onto OP50 plates and embryonic lethality was assayed. N denotes the number of embryos assayed.

**: dpMPK-1 distribution pattern was low. As low dpMPK-1 could arise due to disruption of meiotic progression, we discontinued this analysis

NA: Not applicable, due to sterility

TABLE S2: PHENOTYPES OF DCR-1 TRANSGENES GENERATED via BIOLISTIC TRANSFORMATION

DCR-1 TRANSGENE	GENOTYPE	PHENOTYPES					
		Germline Development		dpMPK-1 Accumulation		Embryo Development	
	Biolistic transformation Transgenes	Phenotype	N (% with phenotype)	Phenotype	N (% with phenotype)	Phenotype	N (% with phenotype)
Null	*dcr-1(ok247)*III	Endomitotic oocytes	50 (100)	high dpMPK-1 in loop	50 (100)	None*	50 (100)
WT	*unc-119(ed3) dcr-1(ok247)*; [pDcr-1::gfp::dcr(WT)::dcr-13'UTR]	WT	52 (100)	WT (bimodal distribution of dpMPK-1 in the germline)	52 (100%)	WT, brood size (218)	52 (100)
S1705E	*unc-119(ed3) dcr-1(ok247);* [pDcr::gfp::dcr(1705E)::dcr-13'UTR]	WT (all oocytes in diakinesis)	28 (100)	WT (bimodal distribution)	28 (100%)	Embryonic lethal (before 30 cell stage)#	89 (100)
S1705A	*unc-119(ed3) dcr-1(ok247;* [pDcr::gfp::dcr(1705A)::dcr-13'UTR]	Pachytene disorganization	39 (100)	low**	ND	Sterile	NA
		Polyploid pachytene nuclei	39 (15)	ND**	ND	NA	
		Disorganized oocytes	39 (100)	ND**	ND	NA	
S1705A/+	*unc-119(ed3) dcr-1(ok247)/ hT2GFP;* [pDcr::gfp::dcr(1705A)::dcr-13'UTR]	Pachytene disorganization	43 (86)	ND**	ND	WT, brood size (30-40) due to low level sterility	NA
		Disorganized oocytes	43 (100)	ND**	ND		
		Polyploid pachytene nuclei	2 (5)	ND**	ND		
S1833E	*unc-119(ed3) dcr-1(ok247;* [pDcr::gfp::dcr(1833E)::dcr-13'UTR]	WT	62 (100)	WT (bimodal distribution of dpMPK-1 in the germline)	62 (100)	Embryonic lethal (before 30 cell stage)#	126 (100)
S1833A	*unc-119(ed3) dcr-1(ok247);* [pDcr::gfpdrc(1833A);;dcr-13'UTR]	WT	88 (87)	high dpMPK-1 in loop	88 (100)	WT, brood size (~180-200)	214 (100)
		Small oocytes	88 (13)	high dpMPK-1 in loop	60 (100)	Sterile	
S1705ES1833E	*unc-119(ed3) dcr-1(ok247);* [pDcr::gfp::dcr(1705E1833E)::dcr-13'UTR]	WT (all oocytes in diakinesis)	14 (100)	WT (bimodal distribution of dpMPK-1 in the germline)	14 (100)	Embryonic Lethal#	39 (100)
S1705AS1833A	*unc-119(ed3) dcr-1(ok247);* [pDcr::gfp::dcr(1705A1833A)::dcr-13'UTR]	Pachytene disorganization	32 (100)	ND**	ND	NA	
		Oocyte Disorganization	32 (100)	ND**	ND	NA	
		Polyploid pachytene nuclei	19 (61)	ND**	ND	NA	

See also Figures 3, 5 and 6

* The animals are sterile and produce no embryos

mothers carrying the embryos were cut open onto OP50 plates and embryonic lethality was assayed. N denotes the number of embryos assayed.

**: dpMPK-1 distribution pattern was low. As low dpMPK-1 could arise due to disruption of meiotic progression, we discontinued this analysis

NA: Not applicable, due to sterility

TABLE S3: MOSAIC ANALYSIS ON DCR-1 PHOSPHO-MUTANT TRANSGENES

DCR TRANSGENE	TISSUE WHERE THE ARRAY IS LOST	PHENOTYPE OBTAINED	
		GERM LINE	EMBRYOS
WT	Soma	Endomitotic Oocytes	Not Obtained
WT	Germ line	Morphologically normal oocytes	inviable
Ser 1705 Ala	Soma	Endomitotic Oocytes*	Not Obtained
Ser 1705 Ala	Germ line	Morphologically normal oocytes*	inviable
Ser 1705 Glut	Soma	Endomitotic Oocytes*	Not Obtained
Ser 1705 Glu	Germ line	Morphologically normal oocytes*	inviable
Ser 1833 Ala	Soma	Endomitotic Oocytes*	Not Obtained
Ser 1833 Ala	Germline	Morphologically normal oocytes*	Inviable
Ser 1833 Glut	Soma	Endomitotic Oocytes*	Not obtained
Ser 1833 Glut	Germ line	Morphologically normal oocytes*	inviable

See also Figure 4

*: The endomitotic oocytes likely arise due to an essentila function of DCR-1 in the soma, and *dcr-1* loss from the germ line (whether wt or mutant) mimics loss of DCR-1 protein, and thus produced similar phenotype

EXPERIMENTAL PROCEDURES.

Protein Alignment

Refseq C terminal Dicer sequences from *C. elegans* (NP_498761, residues 1668-1875), *D. melanogaster* (NP_524453, residues 2018-2220), *Mus musculus* (NP_683750, residues 1675-1877), and humans (NP_803187, residues 1691-1893) were aligned with EXPRESSO (http://www.igs.cnrs-mrs.fr/Tcoffee/tcoffee_cgi/index.cgi) using the mouse Dicer C-terminus (PDB-ID, 3C4B) structure template, and then analyzed with Jalview ver 2.8 (www.jalview.org).

Protein purification and kinase assay

C terminally truncated DCR-1 protein from *C. elegans* (region aa1464-1910) and human, either wild type or alanine mutated at positions 1705 and 1833 in C. elegans or S1712 and S1836 in humans singly or doubly mutated were generated using pTRCHis 6xHIS tag vectors as described (Arur et al., 2009). Induced and His-tag purified recombinant proteins were dialyzed into the kinase assay buffer for 2-4 hours (50 mM Tris-HCl, 10 mM $MgCl_2$, 2 mM DTT, 1 mM EGTA, 0.01 % Brij 35 at pH 7.5). Purified ERK2 kinase was purchased from NEB (cat # P6080L) and reactions carried out as described previously (Arur et al., 2009).

Gonad Dissection, Staining, Image Acquisition and analysis

All animals were dissected 24 hours past L4 stage of development, unless otherwise mentioned. Slides were prepared the day before imaging to allow moisture and air bubbles to dissipate. Each dissected and stained gonad was captured as a montage, with overlapping cell boundaries at 40x magnification. All images were taken on a Zeiss Axio Imager. M2 Upright microscope by using

AxioVs40V 4.8.2.0 microimaging software and a Zeiss Axio MRm camera. The montages were then assembled in Adobe Photoshop CS5.1 and processed identically. Immunoflourscence was performed with anti-GFP antibody prepared in house (Arur and Schedl, 2014; Lopez et al., 2013), anti-MAPKYT (Sigma, (Arur et al., 2009; Lee et al., 2007), and DAPI.

Cell culture analysis

Dicer shRNA (sc-40489-SH) and scrambled shRNA (sc-108060) were obtained from Santa Cruz. FGF2 (233-FB-025/CF) was obtained from R&D Systems. HEK293T cells were infected with either Dicer shRNA or scrambled shRNA according to the manufacturer's protocol. Stable cells were selected by puromycin (7ug/ml) and maintained in DMEM supplemented with 10% FBS. Cells were seeded onto coverslips at 50% confluency and allowed to settle overnight. Cells were then starved for 16hrs before FGF2 stimulation at 50ng/ml for 30min. Cells were fixed with 4% PFA at room temperature, followed by methanol permeabilization at -20^{o}C. After blocking, cells were incubated with either total Dicer or phospho-Dicer antibodies at 1:200 dilution. Secondary antibodies were applied at 1:1000 dilution. Images were collected using the same exposure time for comparison.

For the MEK inhibition assay, HEK293T cells were stimulated with 10ng/ml FGF2 for 30mins, with or without pre-incubation with the 10uM MEK inhibitor U0126. Cells were then lysed and analyzed by western blotting for Dicer phosphorylation status. Tubulin level was used as loading control. Western blotting was performed to assay the effectiveness of the treatment.

Immunofluorescent Staining of mouse uterine tissue

Tissue sections were placed in an oven for 30 min at 55ºC, then deparaffinized and rehydrated. Target antigen retrival was performed in 10mM Sodium Citrate (Fisher Scientific, Cat# S279-3)

in a microwave oven for 20 minutes. Tissues were allowed to cool down to room temperature for 45 minutes. The sections were washed with PBS for 5 minutes, then placed in 3% H_2O_2 for 10 minutes. The sections were washed with PBS for 5 minutes, then incubated in mouse IgG for 1 hour at room temperature. Following the masking of native IgG, the tissue sections were placed in serum-free protein blocking solution made up 3% BSA, 1%Triton-X 100, in PBS for 30 minutes at room temperature. The primary antibodies, anti-phosphoDicer and anti-Dicer were diluted in 10% sheep serum and added directly on top of the tissue sections and incubated overnight at 4ºC. The next day, the tissue sections were washed 3 times with PBS/ 0.1% Tween-20 for 10 minutes to remove non-specific binding. After the washes the sections were incubated with a 1:400 dilution of the secondary antibody (AlexaFluor). The tissue sections were washed 3 times with PBS/ 0.1% Tween-20 for 5 minutes to remove non-specific secondary antibody binding. One drop of Vectashield mounting media (Vector, #H-1200) containing 4', 6-diamidino-2-phenylindole (DAPI) was placed directly on top of each tissue section. The sections were mounted with coverslips with then imaged. *Dicer* was specifically inactivated in Müllerian duct mesenchyme-derived tissues of the reproductive tract of the female mouse, using an *Amhr2-Cre* allele (Gonzalez and Behringer, 2009).

Production of purified wild type and mutant human Dicer for performing the Dicing assay

HEK293T cells were transfected with the various pLVX-hDicer constructs. 36 hours after transduction, cells overexpressing myc-tagged human Dicer proteins were lysed and cleared by centrifugation. hDicer was immunoprecipitated using anti-myc antibody (cell signaling #2278) and immobilized on ProteinA/G-agarose (Santa Cruz SC-2003). The protein was then washed extensively in lysis buffer and stored in PBS supplemented with protease inhibitors (Roche,

#11697498001).

Deep Sequencing Analysis of miRNAs and 26G siRNAs

Total RNA was isolated from 2000 homozygous animals for each genotype. Synchronization of the animals was conducted by an initial L1 arrest (Berkseth et al., 2013) followed by plating the L1 synchronized animals into adult hood. All animals were picked at L4 adult molt and allowed to develop for another 6 hours, 12 hours and 24 hours. At the appropriate time point, 2000 homozygous animals were picked, and washed 3 times with 1X M9 buffer. Total RNA was isolated using TriReagent (Ambion) following manufacturer's instructions. 5' Mono-phosphate bearing small RNAs libraries prepared as described in Lu et al., 2007 (Cheng et al., 2007; Han et al., 2009). The libraries were then shipped to Expression Analysis on the Illumina platform for deep sequencing, and the analysis was performed by Dr. Andrew Fire using the following criteria: The list of germline generated 26G endo siRNA genes from the Kamninga *et al*., (Kamminga et al., 2012) was used and the following criteria was applied to select genes for analysis: a) non repetitive 26G endo siRNA sequences, (b) *eri-1* dependent genes with a minimal of 1.5 fold difference between the oocyte and spermatogenic class, and (c) with a false discovery rate of 0.05.

Western Blot analysis

dcr-1(ok247), DCR-1(WT);*dcr-1(0)*, DCR-1(S1705A);*dcr-1(0)*, DCR-1(S1705E);*dcr-1(0)*, DCR-1(S1833A);*dcr-1(0)*, DCR-1(S1833E);*dcr-1(0)* homozygous hermaphrodites were hand picked (200 for each lane), grown for 24 hours and then harvested for western analysis as previously described (Lee et al., 2007). The extracts were resolved on an 8% SDS-PAGE, transferred to PVDF membrane, and probed with antibodies to GFP and tubulin. Western blots

were developed using SuperSignal West Pico Chemiluminescent Substrate from (Pierce, Rockford, IL), on Kodak BioMax MS films.

SUPPLEMENTAL REFERENCES

Arur, S., Ohmachi, M., Nayak, S., Hayes, M., Miranda, A., Hay, A., Golden, A., and Schedl, T. (2009). Multiple ERK substrates execute single biological processes in Caenorhabditis elegans germ-line development. Proc Natl Acad Sci U S A *106*, 4776-4781.

Arur, S., and Schedl, T. (2014). Generation and purification of highly specific antibodies for detecting post-translationally modified proteins in vivo. Nat Protoc *9*, 375-395.

Berkseth, M., Ikegami, K., Arur, S., Lieb, J.D., and Zarkower, D. (2013). TRA-1 ChIP-seq reveals regulators of sexual differentiation and multilevel feedback in nematode sex determination. Proceedings of the National Academy of Sciences of the United States of America *110*, 16033-16038.

Cheng, L.S., Zha, Z., Xi, J.J., Jiang, B., Liu, J., and Yao, X.B. (2007). [Downregulation of HER2 by adenovirus-mediated RNA interference and its inhibitory effect on growth of SKBR3 breast cancer cell]. Xi Bao Yu Fen Zi Mian Yi Xue Za Zhi *23*, 691-695.

Gonzalez, G., and Behringer, R.R. (2009). Dicer is required for female reproductive tract development and fertility in the mouse. Molecular reproduction and development *76*, 678-688.

Han, T., Manoharan, A.P., Harkins, T.T., Bouffard, P., Fitzpatrick, C., Chu, D.S., Thierry-Mieg, D., Thierry-Mieg, J., and Kim, J.K. (2009). 26G endo-siRNAs regulate spermatogenic and zygotic gene expression in Caenorhabditis elegans. Proceedings of the National Academy of Sciences of the United States of America *106*, 18674-18679.

Kamminga, L.M., van Wolfswinkel, J.C., Luteijn, M.J., Kaaij, L.J., Bagijn, M.P., Sapetschnig, A., Miska, E.A., Berezikov, E., and Ketting, R.F. (2012). Differential impact of the HEN1 homolog HENN-1 on 21U and 26G RNAs in the germline of Caenorhabditis elegans. PLoS Genet *8*, e1002702.

Lee, M.H., Ohmachi, M., Arur, S., Nayak, S., Francis, R., Church, D., Lambie, E., and Schedl, T. (2007). Multiple functions and dynamic activation of MPK-1 extracellular signal-regulated kinase signaling in Caenorhabditis elegans germline development. Genetics *177*, 2039-2062.

Lopez, A.L., 3rd, Chen, J., Joo, H.J., Drake, M., Shidate, M., Kseib, C., and Arur, S. (2013). DAF-2 and ERK couple nutrient availability to meiotic progression during Caenorhabditis elegans oogenesis. Developmental cell *27*, 227-240.